Discharge flow of a bidisperse granular media from a silo: Discrete particle simulations

Y. Zhou,[1,2] P. Ruyer,[1] and P. Aussillous[2,*]

[1]*Institut de Radioprotection et de Sûreté Nuclaire (IRSN), PSN-RES, SEMIA, LIMAR, Cadarache, St Paul-Lez-Durance 13115, France*

[2]*Aix-Marseille Université, CNRS, IUSTI UMR 7343, Marseille 13013, France*

(Received 11 July 2015; revised manuscript received 13 October 2015; published 10 December 2015)

Discrete particle simulations are used to study two-dimensional discharge flow from a silo using both monodisperse and bidisperse mixtures. The density and the velocity profiles through the aperture are measured. In the monodisperse case, two particles' diameters are studied for different outlet diameters. In the bidisperse case, we varied the fine mass fraction of the mixture. In all cases, the density and the velocity profiles are found to follow the same self-similar law. Based on these observations and the previous work of Benyamine *et al.*, a physical model is proposed to describe the flow of bidisperse mixtures giving an explicit expression for the flow rate that is in good agreement with the results.

DOI: 10.1103/PhysRevE.92.062204 PACS number(s): 45.70.Mg, 81.05.Rm

I. INTRODUCTION

The discharge flow of mixtures of particles from silos is of concern to many processes in the food and pharmaceutical industries. It is also of relevance to the ejection of fuel from a typical fuel rod in a nuclear power station during some hypothetical accidental conditions [1]. In most of situations of practical interest, the granular mixture is not monodisperse, however, few studies have been devoted to the discharge flow of a polydisperse mixture. Arteaga and Tüzün [2], followed by Humby *et al.* [3], studied the flow of bidisperse mixtures through a cylindrical and a conical silo. They proposed to describe the behavior of the mixture using the simplest and most used correlation established by Beverloo *et al.* [4] for the discharge of monodisperse granular media from flat-bottomed silos. This correlation is based on dimensional analysis. It supposes that a free-fall arch exists [5], which scales with a reduce outlet length $(D - kd)$ explained by the concept of a useless zone (an empty annulus) for the particles close to the wall [6]. This gives a velocity at the outlet of $v_o \approx \sqrt{g(D - kd)}$ and the flow rate is then

$$Q = C\rho\phi g^{1/2}(D - kd)^{5/2}, \tag{1}$$

where Q is the mass flow rate, g the gravitational acceleration, ρ the particle density, ϕ the particle volume fraction, D the outlet diameter, d the particle diameter, and C and k are fitted parameters. To describe the mixture flow rate, Arteaga and Tüzün proposed to modify this correlation by

$$Q = C\bar{\rho}g^{1/2}(D - \bar{k}\bar{d})^{5/2}, \tag{2}$$

where $\bar{\rho}$ is the mixture density and $\bar{d}$ is a mixture diameter, which characterizes the empty annulus and depends on the fine mass fraction (X_f) and the diameter of the coarse (d_c) and fine particles (d_f),

$$\bar{d} = X_f d_f + (1 - X_f)d_c. \tag{3}$$

The parameter $\bar{k}$ is a fitted coefficient, which is found to depend on the bed microstructure: $\bar{k} = 1.85$ for the coarse continuous phase and $\bar{k} = 1.4$ for the fine continuous phase, where the transition between microstructures depends on the size ratio $(r = d_c/d_f)$.

Recently Benyamine *et al.* [7] performed an experimental study of the discharge flow of a bidisperse granular media from a silo, for a large range of particle diameters, size ratios, and outlet diameters. They proposed a simple physical model to describe the flow of bidisperse mixtures based on the recent experimental work of Janda *et al.* [8] on monodisperse flow. In a two-dimensional (2D) silo, Janda *et al.* found that the velocity and the density profiles at the exit are self-similar, whatever the radius of the aperture $R = D/2$, and wrote $v(x) = v_o[1 - (x/R)^2]^{0.5}$ and $\phi(x) = \phi_o[1 - (x/R)^2]^{0.22}$, where x is the horizontal position. The velocity at the center of the outlet follows,

$$v_o = \sqrt{\gamma g D} \tag{4}$$

with $\gamma = 1.1$, and does not depend on the particle diameters. This scaling of the velocity at the center of the outlet is compatible with the concept of a free fall from a hypothetical arch scaling with D. However, Rubio-Largo *et al.* [9] have shown recently that the free fall arch does not exist as a region below which particles fall solely under gravitational action. Nevertheless, they explained the scaling of the exit velocity based on the acceleration profiles, which collapsed with D.

The variation of density at the center of the outlet depends on the outlet size and on the particle diameter, exhibiting a dilatancy for small aperture in order to maintain the flow of the material. It can be fitted by an asymptotic growth $\phi_o = \phi_\infty[1 - \alpha_1 e^{-D/2\alpha_2}]$, where $\alpha_2 = 3.3d$. Benyamine *et al.* [7] have adapted this concept to their configurations, by assuming that the asymptotic value of the density for big orifices is proportional to the initial bulk volume fraction $(\phi_\infty = \xi\phi_b)$. They wrote that the density at the center of the outlet is given by

$$\phi_o = \xi\phi_b\left[1 - \alpha e^{-\beta\frac{D}{d}}\right] = \xi\phi_b G\left(\frac{d}{D}\right), \tag{5}$$

where $G(d/D) = [1 - \alpha e^{-\beta\frac{D}{d}}]$ is the geometrical factor, which characterizes the dilatancy at the outlet. In the case of bidisperse flow, the model developed by Benyamine *et al.* [7] is based on the three following assumptions.

*pascale.aussillous@univ-amu.fr

(i) For each particle size the density keeps the same self-similar form. Then the density at the center of the outlet can be decomposed into

$$\phi_o = \phi_{of} + \phi_{oc}, \tag{6}$$

where ϕ_{of} and ϕ_{oc} are the fine and coarse density at the center of the outlet, respectively.

(ii) For each particle size, the dilatancy expression [Eq. (5)] is still valid independent of the other particle size,

$$\phi_{oi} = \xi \phi_{bi} G\left(\frac{d_i}{D}\right), \tag{7}$$

for $(i = f,c)$, where $\phi_{bf} = X_f \phi_b$ and $\phi_{bc} = (1 - X_f)\phi_b$ are the fine and coarse initial bulk density, respectively.

(iii) The velocity profile of the mixture keeps its self-similar form, which is independent of the particle diameter [Eq. (4)].

With these hypotheses, Benyamine *et al.* [7] predicted the flow rate of a bidisperse mixture,

$$Q = C'\left[X_f G\left(\frac{d_f}{D}\right) + (1 - X_f) G\left(\frac{d_c}{D}\right)\right] \rho \phi_b \sqrt{gD} S_o, \tag{8}$$

where S_o is the outlet surface. This prediction is found to be in good agreement with their measurements, however, a direct validation of the three presumed hypotheses is not possible in the experimental configuration. To investigate the validity of these assumptions, we performed discrete particle simulations of the discharge flow of granular mixture from a silo.

In the literature, discrete particle simulations have been shown to successfully reproduce the discharge flow of monodisperse granular media from a silo, where Beverloo's correlation is recovered (see Ref. [10] for a review). The current work is devoted to the numerical investigation of the flow in silo discharges using both monodisperse and bidisperse material in a two-dimensional configuration. First the simulated system is described, then we discuss the monodisperse cases and compare our data with the observations of Janda *et al.* [8] on the velocity and density profiles at the outlet. The evolution of these profiles in the bidisperse cases is then studied and compared to the assumptions of Benyamine *et al.* [7]. Finally, a model taking into account these observations is proposed to predict the flow of a bidisperse mixture.

II. SIMULATED SYSTEM

A. System description and numerical settings

To simulate the discharge flow of particles from a silo, we use the LMGC90 software implementation of the contact dynamics method [11]. The particles, interacting through a dense granular flow, are treated as perfectly rigid and inelastic [12]. Contact dissipation is modeled in terms of a friction coefficient that we set to $\mu_p = 0.4$ between particles and to $\mu_w = 0.5$ with the walls.

The two-dimensional silo (Fig. 1) consists of a rectangular tube of height H and width L. The outlet is located at the center of the bottom and has a length D, which was varied.

First, for monodisperse cases, three series of simulations were performed for different disks mean diameter d: using either $d = 2$ mm or $d = 6$ mm, and then using a fixed outlet size $D = 36$ mm (see Table I). To avoid crystallisation a weak polydispersity of $\delta d/d = 0.2$ is introduced. With the particles and aperture available, the number of beads in the aperture (D/d) ranges between 6 and 36. Then, for the bidisperse case, we consider the flow of a binary mixture corresponding to a size ratio of $r = d_c/d_f = 3$ between the coarse particles ($d_c = 6$ mm) and the fine particles ($d_f = 2$ mm) for an outlet size of $D = 36$ mm for various fine mass fractions X_f (see Table II). The number of particles, reported in Tables I and II, was chosen for each simulation to ensure that the discharge flow rate is independent of the column height with $16D < H < 45D$ [13].

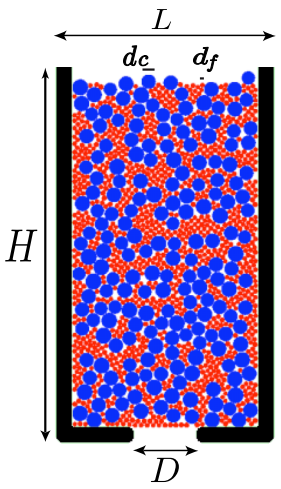

FIG. 1. (Color online) Example of a bidisperse granular media ($X_f = 0.375$) in the silo before the discharge process is initiated.

TABLE I. Simulations performed in the monodisperse case for a fixed particle size ($d = 2$ mm and $d = 6$ mm) or a fixed outlet size ($D = 36$ mm), where N_p is the number of particles and N_t is the number of time steps.

	$d = 2$ mm		$d = 6$ mm	
D/d	N_p	N_t	N_p	N_t
6	5000	17600	4000	34000
8	7500	17600	5400	22000
10	10000	20000	8400	22600
12	11500	16000	12000	22600
14	13500	15000	14000	16000
16	15500	10000	16000	9360
18	20000	5200	18000	8000
20			20000	8000

	$D = 36$ mm	
D/d	N_p	N_t
6.55	4000	27600
7.2	4350	25940
8	5400	26000
9	6750	25000
10.29	9000	20000
12	12000	20230
14.4	16000	5920
36	50000	1692

TABLE II. Simulations performed in the bidisperse case with $d_f = 2$ mm, $d_c = 6$ mm, and $D = 36$ mm, where X_f is the fine mass fraction, N_{pf} and N_{pc} are respectively the number of fine and coarse particles, and N_t is the number of time steps.

X_f	N_{pf}	N_{pc}	N_t
0.125	3500	2722	30000
0.25	7000	2333	25000
0.377	10500	1944	20000
0.5	14000	1555	17516
0.625	17500	1166	9000
0.75	21000	777	6000
0.876	21000	332	6000

To ensure that the lateral walls do not influence significantly the flow, we impose $L = 3D$ [14]. The wall thickness is imposed to be equal to the diameter of the biggest particle in the silo (d_M), with a circular shape at the edge of the outlet (see Fig. 1).

The granular column is prepared by the random deposition of the particles, minimizing the gravitational potential, in the closed silo. A typical bidisperse initial condition is shown in Fig. 1. After the preparation phase, simulations are run with a time step of $\delta t = 5 \times 10^{-4}$ s for the number of time steps N_t reported in Tables I and II. The computational domain is periodic in the vertical direction to keep constant the number of particles. The horizontal boundaries of the computational domain are set at a distance of $10 d_M$ below and above the silo.

B. Numerical statistics and averages

The simulated granular material and its flow are characterized by a set of ensemble-averaged properties that could vary over different time (unsteady) and space (inhomogeneous) scales. From the discrete numerical representation of LMGC90, several averages are computed to study the processes at the scale of the outlet that could govern the steady flow rate at the silo scale.

The bulk volume fraction ϕ_b of a population of particles filling the silo is measured before its discharge. It is obtained by considering the space average of the particle indicator function, whose value is 1 over the spatial extent of particles, and 0 otherwise. This average is calculated over the silo, excluding a region near the boundaries of size D. That corresponds to a sample leading to an accuracy of 5×10^{-3} of the absolute value of ϕ_b.

For bidisperse cases, the mass fraction X_f of the population is defined with respect to the whole set of particles initially in the silo. The bulk particle volume fraction obtained is given in Fig. 2 as a function of the fine mass fraction. As shown in the literature [2], ϕ_b goes through a maximum around $X_f \approx 0.25$, corresponding to dense packing where the fine particles fill the voids between the coarse particles. It can be noted that the fine particles correspond to a packing slightly denser than the coarse particles packing. Finally, the column height is given by $H = S_p/\phi_b L$, where S_p is the total area occupied by particles in the silo.

Let us now consider the discharge. A snapshot of all particle positions is recorded every two time steps. From these snapshots, we first measured globally the instantaneous

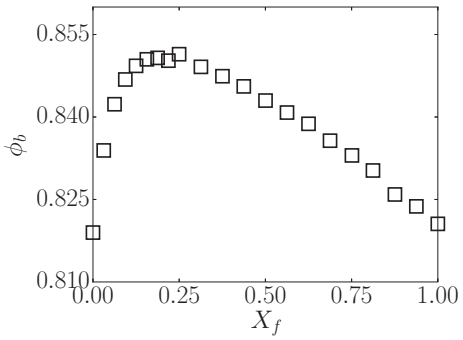

FIG. 2. Bulk particle volume fraction versus the fine mass fraction (X_f) in the bidisperse case (see Table II).

flow rate $Q_i = (\sum_{\delta t} S_p)/\delta t$ corresponding to the surface of particles leaving the silo during a time interval $\delta t = 0.1$s. A typical temporal evolution of the instantaneous flow rate is shown in Fig. 3, where it is found to reach rapidly a rather constant value corresponding to the steady state. The steady flow rate Q is obtained by time averaging the instantaneous flow rate during this steady state.

Then following Janda *et al.* [8], we measured the profile of the particle volume fraction $\phi(x)$ and the velocity $v(x)$ locally at the outlet. These are the average of the statistics performed over the set of snapshots of a computation of a steady flow during, say Δt seconds. Since the studied flow is steady, by ergodicity this time average is equivalent to an ensemble average. For each snapshot, one considers the statistics to be homogeneous over a rectangular domain centered on the measurement location x. The width of this rectangle is $0.2\bar{d}$, where $\bar{d}$ is the mixture diameter defined in Eq. (3), that is actually small with regard to the typical lateral variation of the profiles (that scales with D). The typical length of the ϕ axial variation due to free fall of particles of velocity v is v^2/g. At the outlet of the silo, the velocity v is scaled by $\sqrt{gD}$ and the length scales as D. The height of the rectangular domain is chosen as the outlet wall thickness, which is small with respect to D so that the ergodicity between the space average performed over this square and an ensemble average is valid. The particle volume fraction, $\phi(x)$, is the average over the integration volume (in space and time) of the indicator function of the particles. To reach a relative accuracy ε of the statistical

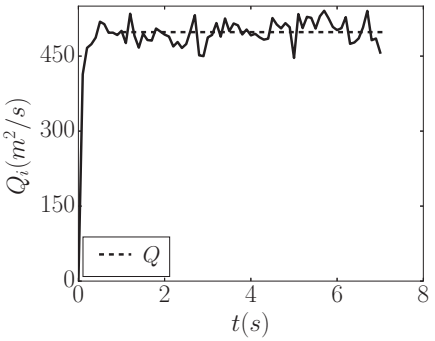

FIG. 3. Temporal evolution of the instantaneous mass flow rate for $d = 2$ mm and $D = 16$ mm in the monodisperse case. The dashed line represents the mean flow rate Q.

estimation of the average value of $\phi(x)$, it is required that Δt be of the order of $\pi\, d^2/(v\ 0.2\bar{d}\ \phi^2\ \varepsilon)$ for particles of size d and velocity v. Scaling v by the average outlet velocity allows for an estimate of the calculation time needed to obtain a given accuracy. In the bidisperse case, these measurements are done for the mixture, but also independently for the coarse and fine particles. It is then obvious that relatively low accuracy will be achieved for the coarse particles when their mass fraction (and therefore ϕ_c) is low in comparison with the accuracy over the fine particles at the same conditions. From the profiles of ϕ, we define the mean outlet value $\bar{\phi}$ as the space average of these profiles over the outlet width D.

The velocity profile at the outlet of a particle population (mixture, fine or coarse) is obtained as the ensemble average (over the same sample) of the individual particle velocity weighted by their volume intersection with the integration domain. It is therefore the space and time average of the product of the indicator function by the individual velocity divided by ϕ. Since standard deviation of the velocity distribution is small, the convergence of statistics toward the average value is more rapid than for ϕ. We checked that the the cross products of the fluctuations is small since $Q \simeq \overline{v}\,\overline{\phi}$.

III. RESULTS AND DISCUSSION

We will now present the simulations results obtained for the discharge of particles from the silo. We will first focus on the monodisperse flow and we will compare our results with those obtained experimentally by Janda *et al.* [8] and numerically by Percier [15] in a similar 2D configuration. These results will be used as a reference for the bidisperse flow studied in the second part.

A. Monodisperse flow

In the monodisperse case, Fig. 4(a) shows the measured particle volume fraction at the outlet, as a function of the horizontal distance from the outlet center, x, for the particles of diameter $d = 2$ mm and for all the outlet diameters simulated. To verify the self-similarity of these profiles, as observed experimentally by Janda *et al.* [8], we chose to normalize the volume fraction by the mean volume fraction, $\bar{\phi}$, to avoid the small scattering visible on the volume fraction in the center of the outlet due to the uncertainty of the measurement. The normalized volume fraction is plotted in Fig. 4(b) versus the horizontal position normalized by the radius of the outlet ($R = D/2$). As expected, the profile is found to be self-similar as the data are all superimposed. Following Janda *et al.* [8] we adjusted the normalized profile by

$$\phi(x) = \bar{\phi}\gamma(\nu_\phi)\left[1 - \left(\frac{x}{R}\right)^2\right]^{\nu_\phi}, \tag{9}$$

where $\gamma(\nu) = (2/\sqrt{\pi})\Gamma(\nu + 3/2)/\,\Gamma(\nu + 1)$ was obtained by integration. The fitting parameter $\nu_\phi = 0.19 \pm 0.01$ is obtained using the least-squares methods and closely matched those reported in previous work [8,15]. We observe exactly the same behavior for the simulations done with the particles of diameter $d = 6$ mm and those with a constant outlet diameter $D = 36$ mm, where all the normalized volume fractions can be adjusted by Eq. (9) with the same power law, $\nu_\phi = 0.19$.

We now turn to the study of the evolution of the mean volume fraction, $\bar{\phi}$, with the parameters of the simulation. Again, following Janda *et al.*, Fig. 4(c) shows the mean volume fraction at the outlet made dimensionless by the bulk volume fraction versus the number of beads in the aperture, D/d, for the three series of monodisperse simulations, $d = 2$ mm (○), $d = 6$ mm (△), and $D = 36$ mm (×). The data superimpose, as observed experimentally by Janda *et al.*, with the mean volume fraction exhibiting an increase from a loose packing for small numbers of beads in the aperture to a tendency to saturate toward 89% of the bulk volume fraction for large numbers. The data are well represented by the expression of Janda *et al.* (see the full line in the figure),

$$\bar{\phi} = \xi_\phi \phi_b\left[1 - \alpha e^{-\beta \frac{D}{d}}\right] = \xi_\phi \phi_b G\left(\frac{d}{D}\right), \tag{10}$$

with the fitting parameters $\xi_\phi = 0.89$, $\alpha = 0.45$, and $\beta = 0.13$ (obtained using the least-squares method), which closely match those reported in previous work [8,15]. We note that $G(d/D) = [1 - \alpha e^{-\beta \frac{D}{d}}]$, the function that depends on the number of beads in the aperture and characterizes the dilatancy at the outlet due to the geometrical constraint.

In the same way, the profiles of the vertical component of the velocity, $v(x)$, and the profiles of the horizontal component of the velocity, $u(x)$, for the particles of diameter $d = 2$ mm are

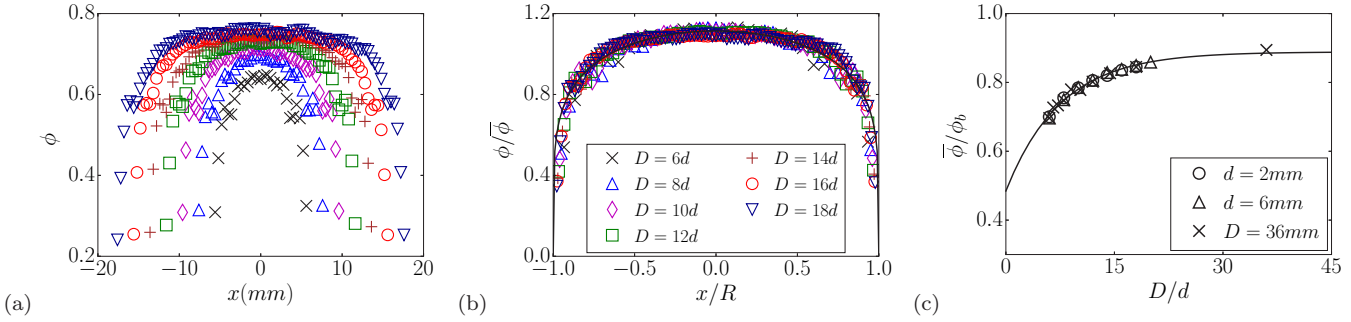

FIG. 4. (Color online) Monodisperse flow of particles of diameter of $d = 2$ mm for different outlet diameters. (a) Horizontal profiles of the volume fraction versus the position (x). (b) Horizontal profiles of the volume fraction normalized by the mean volume fraction ($\bar{\phi}$) versus the position normalised by the outlet radius ($R = D/2$). The full line represents Eq. (9) with $\nu_\phi = 0.19$. (c) Mean volume fraction at the outlet ($\bar{\phi}$) normalized by the bulk volume fraction (ϕ_b) versus the outlet diameter normalized by the particle diameter (D/d), for the three series of monodisperse simulations. The full line represents Eq. (10) with $\xi_\phi = 0.89$, $\alpha = 0.45$, and $\beta = 0.13$.

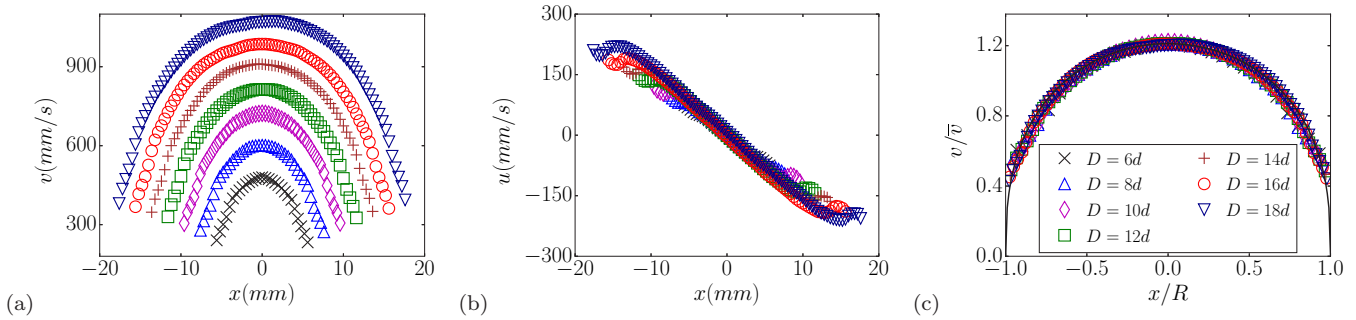

FIG. 5. (Color online) Monodisperse flow of particles of diameter of $d = 2$ mm for different outlet diameters. (a) Horizontal profiles of the vertical velocity v. (b) Horizontal profiles of the horizontal velocity u. (c) Horizontal profiles of the vertical velocity made dimensionless by the mean vertical velocity ($\bar{v}$) versus the position normalized by the outlet radius ($R = D/2$). The full line represents Eq. (11) with $\nu_v = 0.38$.

plotted, respectively, in Figs. 5(a), 5(b). The vertical velocity profiles are quasiparabolic and depend on the outlet diameter, whereas the horizontal velocity profile is found to be mainly linear. These profiles show that the flow out of the silo is not fully vertical but has a horizontal component towards the center. It is interesting to note that the horizontal profiles seem to be nearly self-similar without any normalization, whereas the vertical profiles present a self-similarity when normalized by the mean velocity as a function of the horizontal position made dimensionless by the radius of the outlet, see Fig. 5(c). Following Janda *et al.* [8], we have adjusted the vertical profile by

$$v(x) = \bar{v}\gamma(\nu_v)\left[1 - \left(\frac{x}{R}\right)^2\right]^{\nu_v}, \qquad (11)$$

with the fitting parameter $\nu_v = 0.38 \pm 0.01$ obtained using the least-squares method. This coefficient, similar to that obtained numerically in a 2D discrete simulation by Percier [15], is slightly lower than that obtained experimentally by Janda *et al.* ($\nu_v = 0.5$). This may be explained by the difference in the geometries between the simulations, corresponding to a column of disks, and the experiments, corresponding to a column of one layer of spheres between two plates. Again, we observe exactly the same behavior for the simulations done with the particles of diameter $d = 6$ mm and those with a constant outlet diameter $D = 36$ mm, where all the normalized vertical velocities can be adjusted by Eq. (11) with the same power law, $\nu_v = 0.38$.

Following Janda *et al.*, the evolution of the mean vertical velocity $\bar{v}$ is plotted in Fig. 6(a) versus the outlet radius for the three series of simulations in the case of monodisperse flow, corresponding to constant particle diameters $d = 2$ mm ($\circ$) and $d = 6$ mm ($\triangle$) or constant outlet diameter $D = 36$ mm ($\times$). The collapse of the data is not completely satisfactory and the adjustment by a square root law is not as fair as expected (see the full line in the figure corresponding to $\bar{v} = 1.46\sqrt{gD}$). It seems in our simulation that the particle diameter plays a role in the determination of the mean vertical velocity. This is particularly visible for the data corresponding to a constant outlet diameter ($\times$) where the velocity is not constant when the particle diameter varies.

To take this role into account, we have plotted in Fig. 6(b) the mean velocity made dimensionless by $\sqrt{gd}$ versus the number of beads in the aperture D/d. In this representation, the data collapse in a single curve. To be consistent with the asymptotic value and with the observations made on the mean volume fraction, we have adjusted the mean vertical velocity by

$$\bar{v} = \xi_v\sqrt{gD}\left[1 - \alpha e^{-\beta\frac{D}{d}}\right] = \xi_v\sqrt{gD}G\left(\frac{d}{D}\right) \qquad (12)$$

with the fitting parameter $\xi_v = 1.55$ and the same fitting parameters in the geometrical function $G(d/D)$ as the ones obtained for the volume fraction. This suggests that the same physical mechanism is responsible for the reduction in the

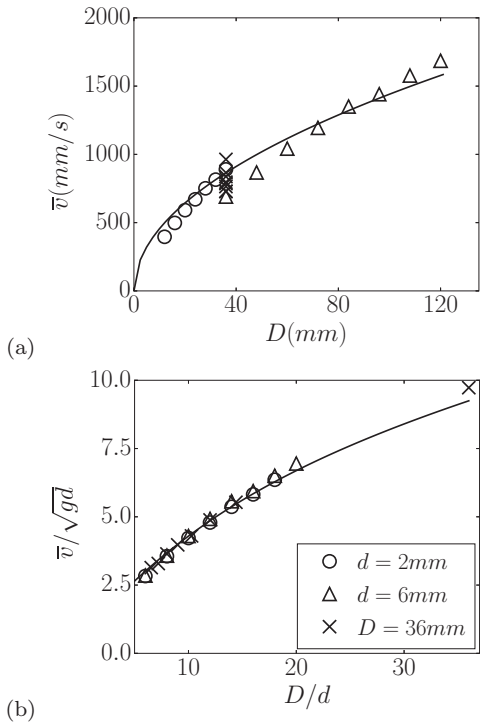

FIG. 6. (a) Mean vertical velocity versus the length of the aperture D. The full line represents the best fit with a square root law, $\bar{v} = 1.46\sqrt{gD}$. (b) Mean vertical velocity made dimensionless by $\sqrt{gd}$ versus the number of beads in the apertures D/d. The full line represents Eq. (12) with $\xi_v = 1.55$, $\alpha = 0.45$, and $\beta = 0.13$.

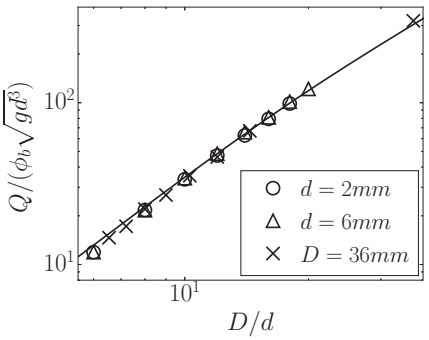

FIG. 7. Flow rate made dimensionless by $\sqrt{gd^3}$ versus the number of beads in the aperture D/d. The full line represents Eq. (13) with $C = 1.42$.

mean velocity and the mean volume fraction at the outlet when the number of beads in the aperture decreases, which is consistent with a continuous description of the granular media throughout the silo, even close to the outlet [9,16].

Finally, we can deduce, from Eqs. (9)–(12), the discharge flow rate of monodisperse beads from a two-dimensional silo,

$$Q = \int_{-D/2}^{D/2} \phi(x)v(x)dx = C\left[G\left(\frac{d}{D}\right)\right]^2 \phi_b\sqrt{gD^3}, \quad (13)$$

where $C = \xi_\phi\xi_v\gamma(v_v)\gamma(v_\phi)\int_0^1(1-t^2)dt = 1.42$.

In Fig. 7, the measured flow rate made dimensionless by $\sqrt{gd^3}$ is plotted versus the number of beads in the aperture D/d for the three series of simulations (constant particle diameters $d = 2$ mm, ○, and $d = 6$ mm, △, or constant outlet diameter $D = 36$ mm, ×). We recover the classical result corresponding to a collapse of the data on a single curve, which is in excellent agreement with Eq. (13) with $C = 1.42$ (see the full line in the figure). As pointed out by Janda *et al.* [8], the precise knowledge of the profiles of the volume fraction and velocity of particle through the outlet allow an accurate prediction of the flow rate, based on physical observations. The monodisperse study will be used in the following as a reference for the bidisperse flow.

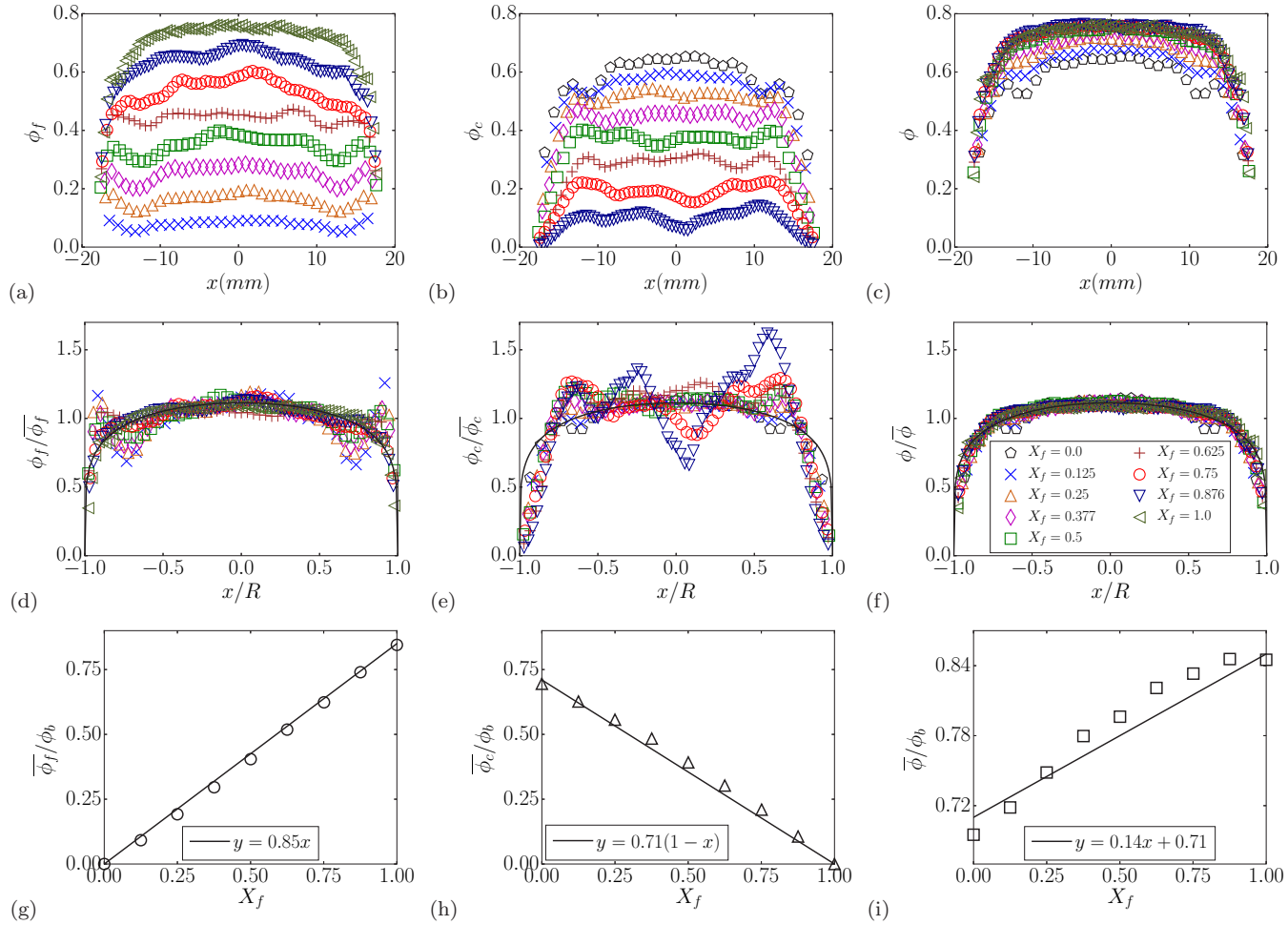

FIG. 8. (Color online) Flow of a bidisperse mixture with $d_f = 2$ mm and $d_c = 6$ mm for an outlet length $D = 36$ mm, for different fine mass fractions: horizontal profiles of the volume fraction for (a) the fine particles, (b) the coarse particles, and (c) the mixture. Horizontal profile of the volume fraction made dimensionless by the mean volume fraction, versus the horizontal position normalised by the radius of the outlet, for (d) the fine particles, (e) the coarse particles, and (f) the mixture. The full line represents Eq. (9) with $\nu_\phi = 0.19$. Mean volume fraction at the outlet $\bar{\phi}$ normalised by the bulk volume fraction (ϕ_b) versus the fine mass fraction X_f, for (g) the fine particles, (h) the coarse particles, and (i) the mixture. The full lines represent respectively, Eqs. (16), (17), and (18).

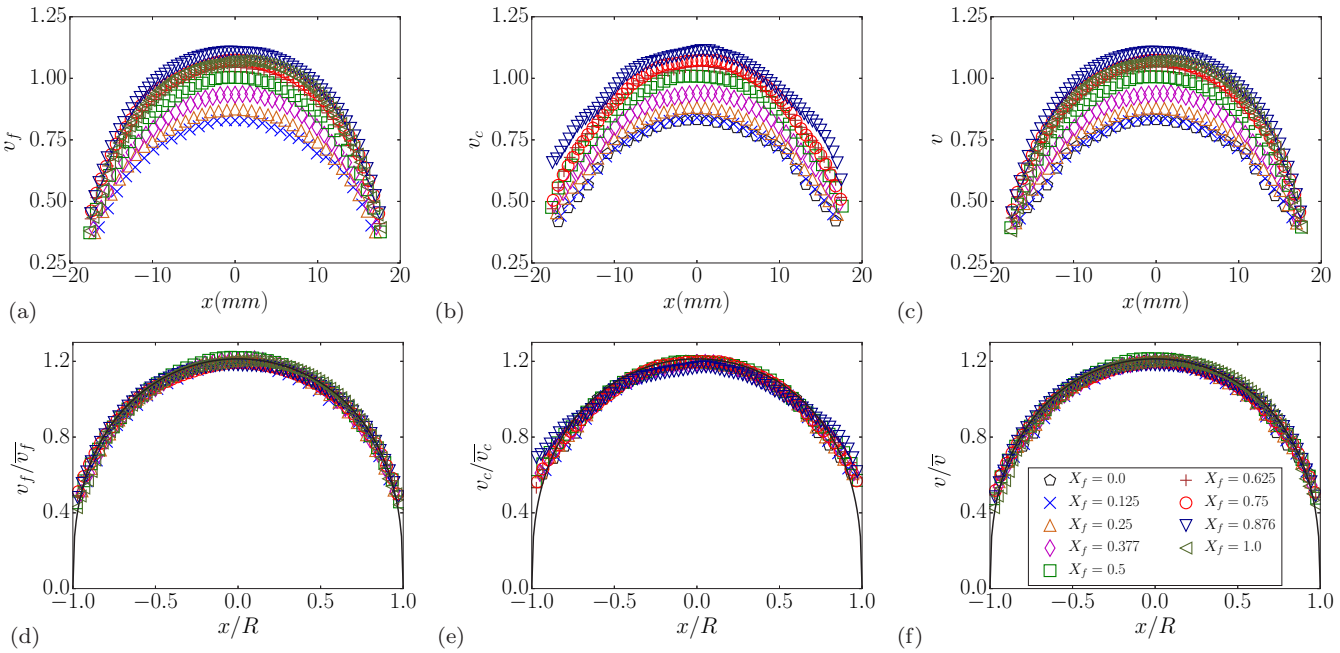

FIG. 9. (Color online) Flow of a bidisperse mixture with $d_f = 2$ mm and $d_c = 6$ mm for an outlet length $D = 36$ mm, for different fine mass fractions: horizontal profiles of the vertical velocity for (a) the fine particles, (b) the coarse particles, and (c) the mixture. Horizontal profiles of the vertical velocity normalized by the mean vertical velocity, versus the horizontal position normalized by the radius of the outlet, for (d) the fine particles, (e) the coarse particles, and (f) the mixture. The full line represents Eq. (11) with $\nu_v = 0.38$.

B. Bidisperse flow

To predict the flow of a bidisperse mixture from a silo, Benyamine *et al.* [7] have developed a model based on three assumptions. The measurement of the horizontal profile of the volume fraction and the velocity at the outlet of both the fine and coarse particles will enable testing of these assumptions, one by one.

(i) In their model, Benyamine *et al.* first assumed that for each particle size the volume fraction keeps the same self-similar form. In the case of the flow of bidisperse mixture with $d_f = 2$ mm and $d_c = 6$ mm for an outlet length $D = 36$ mm, Figs. 8(a), 8(b) show the horizontal profile of the volume fraction for various fine mass fractions, X_f, for the fine and coarse particles. These profiles are found to be self-similar when normalized by the mean volume fraction as shown in Figs. 8(d), 8(e), and they correspond to the prediction of Eq. (9), with $\nu_\phi = 0.19$ as for the monodisperse case (full line in the figures). The first condition is consequently fulfilled, which is demonstrated by the fact that horizontal profile of the volume fraction of the mixture follows the same self-similarity as can be seen in Figs. 8(c), 8(f). Subsequently the mean volume fraction at the outlet can be decomposed into

$$\bar{\phi} = \bar{\phi}_f + \bar{\phi}_c, \tag{14}$$

where $\bar{\phi}_f$ and $\bar{\phi}_c$ are respectively the fine and coarse mean volume fraction at the outlet.

(ii) Second, they assumed that for each particle size, the dilatancy expression obtained in the monodisperse case is still valid independently of the other particle size,

$$\bar{\phi}_i = \xi_\phi \phi_{bi} G\left(\frac{d_i}{D}\right), \tag{15}$$

for $(i = f,c)$. Considering that the fine and coarse initial bulk density are respectively given by $\phi_{bf} = X_f \phi_b$ and $\phi_{bc} = (1 - X_f)\phi_b$, implies that

$$\bar{\phi}_f = X_f \phi_b \xi_\phi G\left(\frac{d_f}{D}\right), \tag{16}$$

$$\bar{\phi}_c = (1 - X_f)\phi_b \xi_\phi G\left(\frac{d_c}{D}\right), \tag{17}$$

$$\bar{\phi} = \phi_b \xi_\phi \left[X_f G\left(\frac{d_f}{D}\right) + (1 - X_f) G\left(\frac{d_c}{D}\right)\right]. \tag{18}$$

These predictions are compared to the results obtained from the simulations in Figs. 8(g)–8(i) where the mean volume fraction at the outlet ($\bar{\phi}$) normalized by the bulk volume fraction (ϕ_b) is plotted versus the fine mass fraction X_f, respectively for the fine particles, the coarse particles and the mixture. The agreement is found to be fairly good, which validates this second hypothesis.

(iii) Finally, they assumed that the velocity profile of the mixture keeps its self-similar form, which is independent of the particle diameter. However, in our simulation the velocity profile for the monodisperse case is found to depend on the number of particles in the aperture. Nevertheless, Fig. 9 shows that the vertical profile in the bidisperse case for the fine particles, the coarse particles and the mixture retain their self-similar form if normalized by the mean vertical velocity. Again, Eq. (11), with $\nu_\phi = 0.38$, found for the monodisperse case fits the data very well.

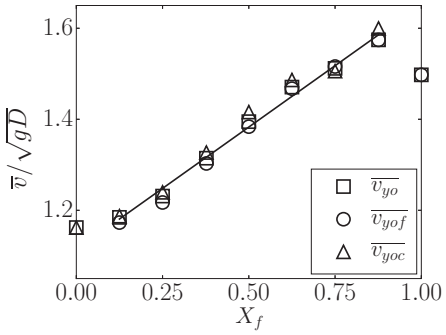

FIG. 10. Mean velocity of the fine particles (○), the coarse particles (△), and the mixture (□) versus the fine mass fraction X_f. The full line represents the best linear fit excluding the pure cases ($X_f = 0$ and 1).

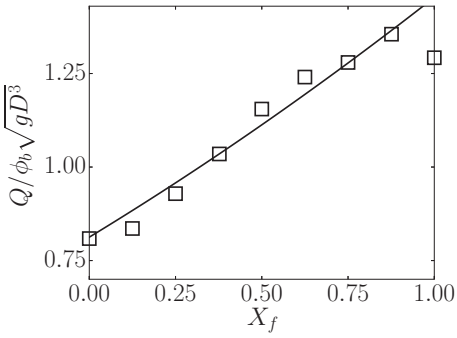

FIG. 11. Flow rate Q made dimensionless by $\phi_b\sqrt{gD^3}$ versus the fine mass fraction X_f in the bidisperse case. The full line represents a linear fit excluding the monodisperse cases given in Eq. (19).

Figure 10 shows the mean velocity versus the fine mass fraction for the fine particles (○), the coarse particles (△), and the mixture (□). The important finding exhibited in this figure is that the velocity of the fine and coarse particle are identical for a given fine mass fraction. This means that the mixture behaves as a continuous media with $\bar{v}(X_f) = \bar{v}_f(X_f) = \bar{v}_c(X_f)$. This also implies that there is no segregation for our conditions. Moreover the data, excluding the monodisperse cases, seems to follow a linear trend,

$$\bar{v}/\sqrt{gD} = \xi_v[1.07X_f + 0.72(1 - X_f)] = \xi_v K(X_f); \quad (19)$$

see the full line in the figure. These observations suggest that the spatial arrangement of the grains close to the outlet is the single feature that depends on the size distribution of the granular material. In this hypothesis, the different behavior of the monodisperse case could correspond to a specific arrangement when the mixture is monosized. A future work on the spatial organization of the grains near the outlet should test this hypothesis.

Finally, using Eqs. (14)–(19), we obtain a new formula to describe the discharge flow rate bidisperse beads from a two-dimensional silo,

$$Q = CK(X_f)\left[X_f G\left(\frac{d_f}{D}\right) + (1 - X_f)G\left(\frac{d_c}{D}\right)\right]\phi_b\sqrt{gD^3}, \quad (20)$$

where $C = 1.42$ corresponds to the same prefactor as in Eq. (13). This equation is plotted in Fig. 11 and is found to be in good agreement with the results of the numerical simulations.

IV. CONCLUSION

We have numerically studied the discharge flow of both monodisperse and bidisperse mixtures of disks from a two-dimensional silo using discrete particle simulations in the stationary regime. The density and the velocity profiles through the aperture were measured, in the monodisperse case for two particles' diameters, varying the outlet diameters, and for one outlet diameter, varying the particle diameters. In the bidisperse case both profiles are measured for each species and for the mixture.

In the case of monodisperse particles, we recovered most of the experimental observations of Janda *et al.* [8]. The density and the velocity profiles are found to follow a given self-similar law in the whole range of parameters. The mean density at the outlet exhibits a dilatancy depending on the number of beads in the aperture. However, contrary to Janda *et al.* [8], the mean vertical velocity is found to depend also on the number of beads in the aperture, with the same geometrical factor as the mean density.

In the case of the bidisperse particles, we validated the hypothesis developed previously by Benyamine *et al.* [7] on the density to predict the flow rate of the bidisperse granular media from a silo. We found that the horizontal profiles of the density of the fine particles, the coarse particles and the mixture, keep the same self-similarity as for the monodisperse case, whatever the fine mass fraction. Then, we showed that the dilatancy expression is still valid for each particle size, independent of the other particle size. Finally, the model of Benyamine *et al.* assumes that the particle velocities at the outlet are the same whatever the particle diameters. As the velocity depends on the particle diameters, this hypothesis is not fulfilled. However, we observed that the velocity profiles follow the same self-similarity as for the monodisperse case. For a given fine mass fraction, we observed that the mixture behaves as a continuous media with the same mean velocity for each species and the mixture. We found that the mixture velocity is roughly proportional to the fine mass fraction. Based on all of these hypothesis, we proposed an expression for the flow rate of a bidisperse mixture [Eq. (20)], which is in good agreement with our simulation data.

Our results suggest that during the discharge flow of a silo the bidisperse mixture can be seen as a continuous media even close to the outlet, as pointed out recently in the case of monodisperse flow [9,16]. The dilatancy of the mixture at the outlet plays a major role in the dependance of the flow rate with the particle size.

ACKNOWLEDGMENTS

We would like to thank R. Mozul and F. Perales for assistance with LMGC90, and J.E. Butler for a critical reading.

[1] A. Martin, Thesis, Université Montpellier II - Sciences et Techniques du Languedoc, 2010 (unpublished).
[2] P. Arteaga and U. Tüzün, Chem. Eng. Sci. **45**, 205 (1990).
[3] S. Humby, U. Tüzün, and A. B. Yu, Chem. Eng. Sci. **53**, 483 (1998).
[4] W. A. Beverloo, H. A. Leniger, and J. V. de Velde, Chem. Eng. Sci. **15**, 260 (1961).
[5] B. Tighe and M. Sperl, Granul. Matter **9**, 141 (2007).
[6] R. L. Brown and J. C. Richards, Trans. Instn. Chem. Engrs. **38**, 243 (1960).
[7] M. Benyamine, M. Djermane, B. Dalloz-Dubrujeaud, and P. Aussillous, Phys. Rev. E **90**, 032201 (2014).
[8] A. Janda, I. Zuriguel, and D. Maza, Phys. Rev. Lett. **108**, 248001 (2012).
[9] S. M. Rubio-Largo, A. Janda, D. Maza, I. Zuriguel, and R. C. Hidalgo, Phys. Rev. Lett. **114**, 238002 (2015).
[10] H. Zhu, Z. Zhou, R. Yang, and A. Yu, Chem. Eng. Sci. **63**, 5728 (2008).
[11] F. Dubois, M. Jean, M. Renouf, R. Mozul, A. Martin, and M. Bagneris, 10e colloque national en calcul des structures, May 2011, Giens, France (unpublished).
[12] F. Radjai and F. Dubois, *Discrete-element modeling of granular materials* (Wiley-Iste, London, 2011), p. 425.
[13] D. Hirshfeld and D. Rapaport, Eur. Phys. J. E **4**, 193 (2001).
[14] R. M. Nedderman, U. Tuzün, S. B. Savage, and G. T. Houlsby, Chem. Eng. Sci. **37**, 1597 (1982).
[15] B. Percier, Thesis, Université Lyon I - ENS de Lyon, 2013 (unpublished).
[16] L. Staron, P.-Y. Lagrée, and S. Popinet, Phys. Fluids **24**, 103301 (2012).